Supporting Information for

Multifunctional Sulfur-Mediated Strategy Enabling Fast-Charging Sb_2S_3 Micro-Package Anode for Lithium-Ion Storage

Shaohua Wang[a,b], Yong Cheng[a,*], Hongjin Xue[a,b], Wanqiang Liu[d], Zheng Yi[a,**], Limin Chang[c,***], Limin Wang [a,b]

[a]State Key Laboratory of Rare Earth Resource Utilization, Changchun Institute of Applied Chemistry, CAS, Changchun, 130022, China.

[b]School of Applied Chemistry and Engineering, University of Science and Technology of China, Hefei, 230026, China.

[c]Key Laboratory of Preparation and Applications of Environmental Friendly Materials (Jilin Normal University), Ministry of Education, Changchun, 130103, China.

[d]School of Materials Science and Engineering, Changchun University of Science and Technology, Changchun, 130022, China.

E-mail: cyong@ciac.ac.cn; yizheng@ciac.ac.cn; lmchang@jlnu.edu.cn

Experimental Section

Chemicals. All the reagents are of analytical grade and used without further purification. Analytically pure antimony trioxide (Sb_2O_3, Aladdin, China), sulfur (S, Tianjin Guangfu Reagent Company, China), expandable graphite (Nanjing Xianfeng, China). The $LiNi_{1/3}Co_{1/3}Mn_{1/3}O_2$ (NCM 333) was purchased from Beijing Dangsheng Material Technology Co., Ltd.

Preparation of EG. The expandable graphite was annealed at 1000℃ for 1 min under argon atmosphere with the heating rate of 5℃/min to obtain EG.

Preparation of Sb_2S_3@EG'-S, Sb_2S_3/EG- S, EG-S-30, EG-30 composite material. Sb_2O_3, EG, and S are mixed with ball-milling in the weight ratio of 3:1:5. Planetary ball mill was used with a ball-to-material ratio of 50:1, a speed of 400 r/min, and ball-milling time of 30h. The final material was collected and annealed at 500℃ for 2 hours in a tube furnace under argon atmosphere with the heating rate of 2℃/min. Then, the Sb_2S_3@EG'-S composite material was obtained. As comparison, Sb_2S_3/EG-S composite material was prepared by just introducing the sulfur in the annealing process. The preparation method of EG-S-30 and EG-30 is the same as Sb_2S_3@EG'-S and Sb_2S_3/EG- S except the Sb_2O_3 is absence.

Materials characterizations. The crystalline phases of the as-prepared samples were investigated by X-ray diffraction (XRD) on a Bruker D8 Focus power X-ray diffractometer with Cu Kα radiation (λ=0.154056 nm) at a scan rate of 5°min^{-1} in the 2θ range of 10~80°. The morphologies and microstructures of the as-synthesized products were observed by a field-emission scanning electron microscope (FE-SEM,

Hitachi S-4800) with an acceleration voltage of 10 kV. Detailed microstructure analysis was conducted using a transmission electron microscopy (TEM, Tecnai G2) with a field emission gun operating voltage of 200 kV. Thermo-gravimetric (TG) analysis was carried out to estimate the carbon content on an STA 449 Jupiter (NETZSCH) thermogravimetry analyzer from room temperature to 800°C with a heating rate of 10°C min^{-1}. X-ray photoelectron spectra (XPS) analysis was performed to evaluate the surface state and chemical composition on an ESCALABMKLL X-ray photoelectron spectrometer using an Al Kα source. Nitrogen adsorption/desorption isotherms were acquired through a Micromeritics ASAP 2010 surface area and porosity analyzer at -196°C. The specific surface area was calculated by using the Brunauer-Emmett-Teller (BET) method. The pore size distribution profile was derived via a nonlocal density functional theory (DFT) method from the adsorption branch of the nitrogen adsorption/desorption isotherms.

Electrochemical measurements. Coin-type cells were assembled in an argon-filled glove box to investigate the lithium storage performances of the as-prepared samples. For the preparation of the working electrode, a homogenous slurry was acquired by mixing the as-prepared samples, acetylene black and carboxymethyl cellulose (CMC) with a mass weight ratio of 80:10:10 dissolving in appropriate deionized water. The resultant slurry was then coated onto a copper foil and dried in a vacuum oven at 60 °C overnight. The average mass loading was 1.0~1.3 mg cm^{-2}. The half cells were constructed by using the lithium foil as the counter/reference electrode, Celgard 2400 membrane as the separator, and 1 M $LiPF_6$ dissolved in ethylene carbonate (EC) and

diethyl carbonate (DEC) (1/2, v/v) with 10 % (v) addition of fluoroethylene carbonate (FEC) as the electrolyte. For Li-ion full cells, commercial $LiNi_{1/3}Co_{1/3}Mn_{1/3}O_2$ (NCM 333) (91 wt.%), C45 (2 wt.%), KS-6 (2 wt.%) and polyvinylidene fluoride (PVDF, 5 wt.%) were mixed in N-methyl-2-pyrrolidone (NMP) and then pasted onto a piece of Al foil to form the cathode electrode. In addition, the NCM 333 mass loading of the cathode was appropriately chosen to balance the capacity of the anode. The specific capacity of the full cell is calculated according to the mass of the cathode electrode. The anode was electrochemically pre-lithiated for five cycles in order to eliminate the irreversible capacity in the first cycle before being used. The galvanostatic charge/discharge performance was tested on a programmable battery testing instrument (LAND CT2001A) at room temperature. Cyclic voltammogram (CV) and electrochemical impedance spectroscopy (EIS) measurements were carried out on a Bio-Logic VMP3 Electrochemical Workstation.

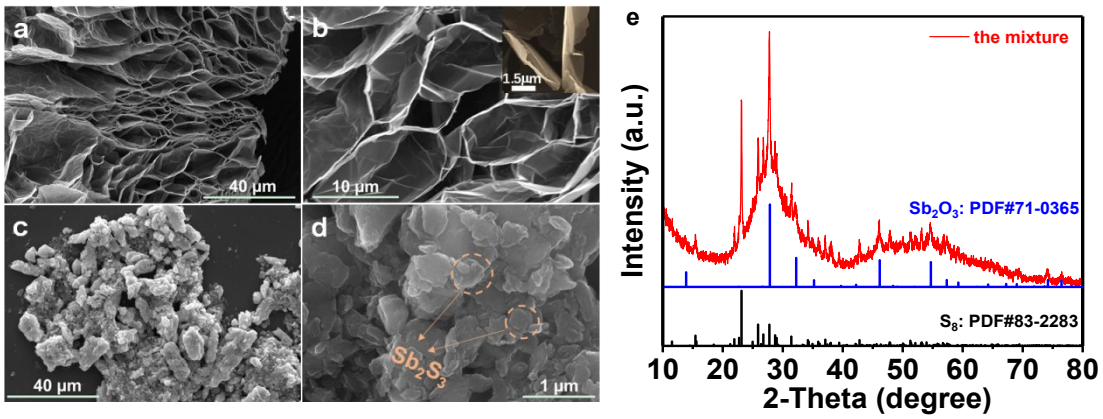

Figure S1. SEM images of (a, b) EG and (c, d) Sb_2S_3/EG-S. (e) XRD pattern for the mixture before annealed.

a

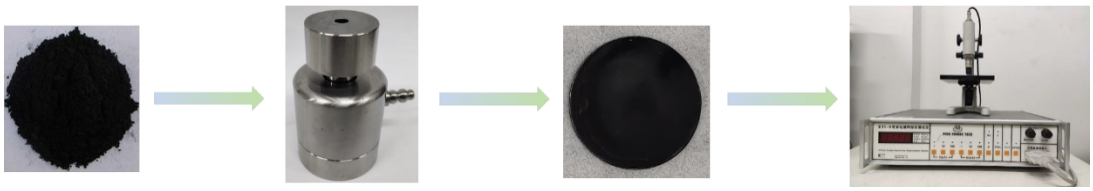

b

	EG-S-30	EG-30
1 st	19.23 S cm^{-1}	0.055 S cm^{-1}
2 nd	19.23 S cm^{-1}	0.054 S cm^{-1}
3 rd	19.05 S cm^{-1}	0.052 S cm^{-1}
Average value	19.17 S cm^{-1}	0.0536 S cm^{-1}

Figure S2. (a) Schematic diagram of four-probe method to measure the conductivity of EG-S-30 and EG-30 material. (b) The conductivity of two samples.

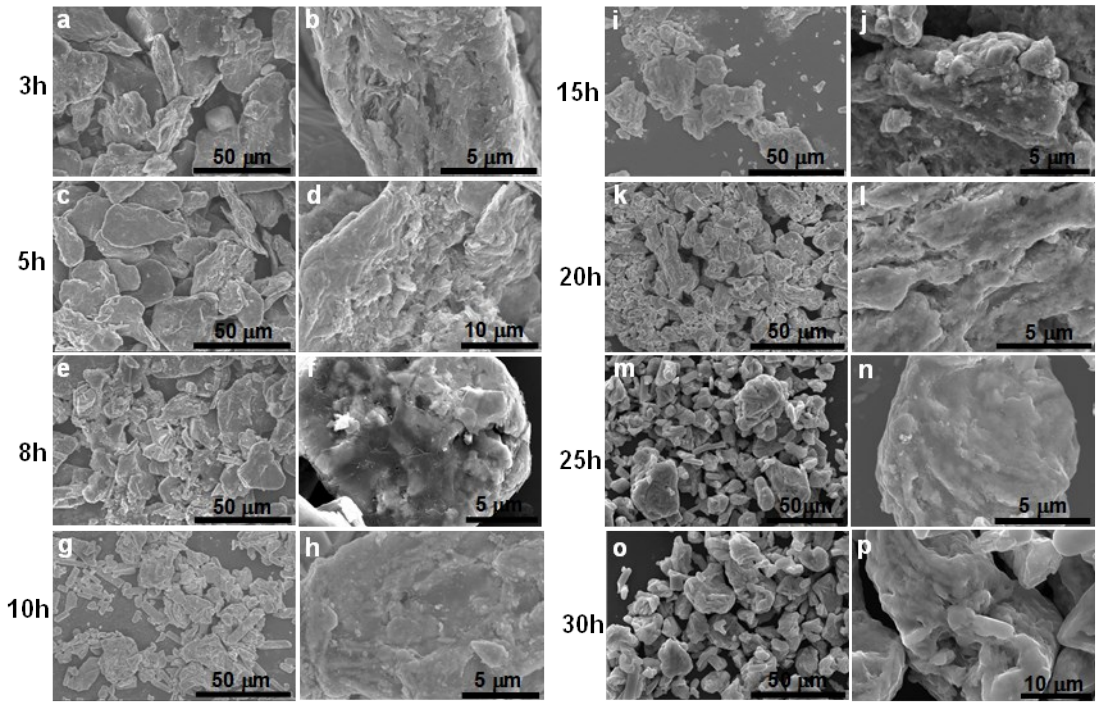

Figure S3. SEM images of Sb_2S_3@EG'-S material at different balling time.

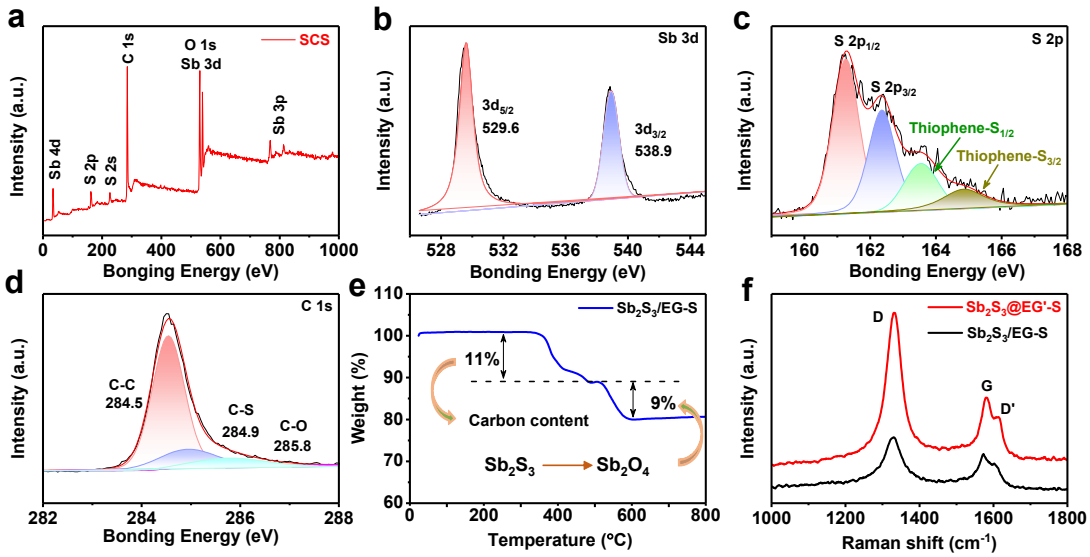

Figure S4. X-ray photoelectron spectroscopy (XPS): (a) survey, (b) Sb 3d, (c) S 2s, (d) C 1s of Sb_2S_3/EG-S. (e) TG curve. (f) Raman spectra of Sb_2S_3@EG'-S and Sb_2S_3/EG-S

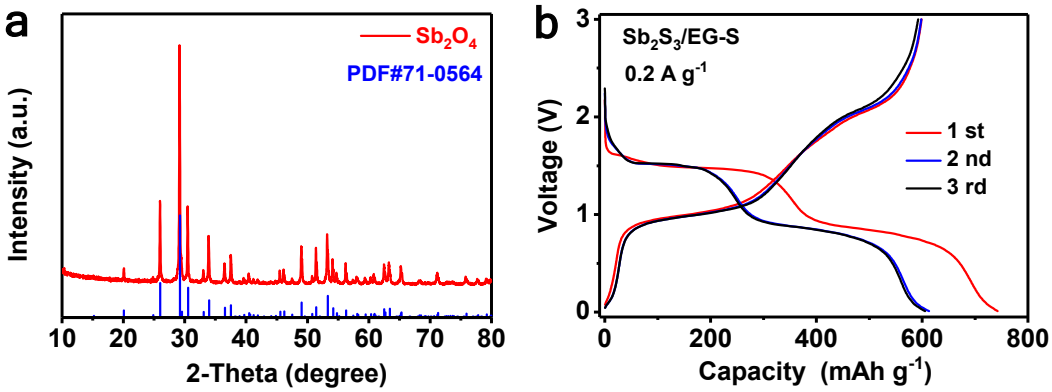

Figure S5. (a) XRD pattern of the samples after completed annealed. (b) Charge/discharge curves of Sb_2S_3/EG-S anode at the current density of 0.2 A g^{-1}.

Table S1. The peak potential and displacement of Sb_2S_3@EG'-S anode and Sb_2S_3/EG-S anode in dQ/dV curves at the current density of 5 C.

	0.01-1.5 V		1.5-3 V	
	Sb_2S_3@EG'-S	Sb_2S_3/EG-S	Sb_2S_3@EG'-S	Sb_2S_3/EG-S
1 st-0.2C	0.98 V	0.982 V	2.082 V	2.060 V
10 th-5C	1.0 V	1.124 V	2.106 V	2.248 V
50 th-5C	1.018 V	1.124 V	2.123 V	2.234 V
100 th-5C	1.043 V	1.159 V	2.084 V	2.277 V
120 th-5C	1.045 V	1.223 V	2.08 V	2.299 V
$\Delta V(V_{120}-V_{10})$	-0.045 V	0.099 V	-0.026 V	0.051 V

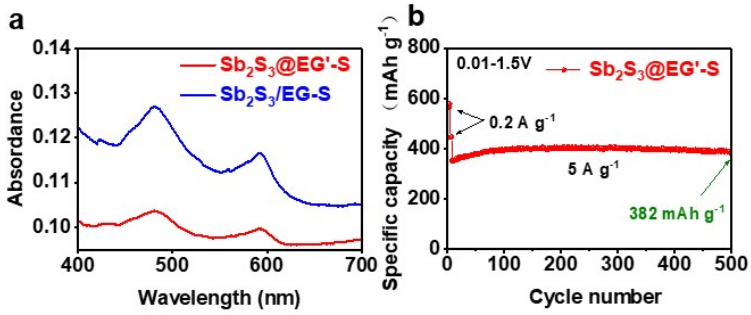

Figure S6. (a) ultraviolet absorption spectrum of Sb_2S_3@EG'-S anode and Sb_2S_3/EG-S anode. (b) Cycle performance of Sb_2S_3@EG'-S anode at the current density of 5 A g^{-1} (The voltage range is 0.01 to 1.5V).

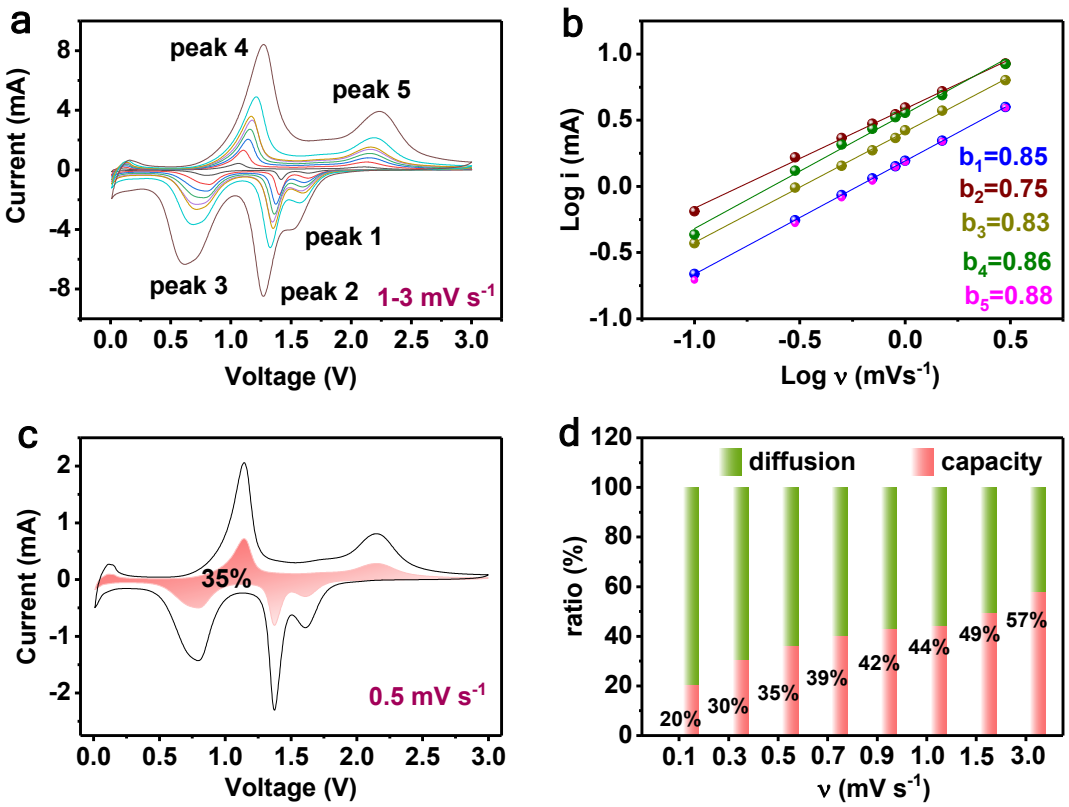

Figure S7. (a) CV curves of the Sb_2S_3@EG'-S electrode at different scan rates. (b) Relationship between the logarithm cathodic peak current and logarithm scan rates. (c) Capacitive contribution (pink) and diffusion contribution at the scan rate of 0.5 mV s^{-1}. (d) Normalized contribution ratio of capacitive capacities at different scan rates.

Table S2. Comparison of the electrochemical performance of as-prepared Sb_2S_3@EG'-S and those Sb_2S_3-based anodes reported before.

Materials	Mathod	Current Density (mAh g^{-1})	Specific Capacity (mAh g^{-1})	Cycle number	Ref.	Year
This work (micro-package Sb_2S_3@EG'-S)	ball-milling	1000 5000 15000	645.5 548 444	120 100 /		/
Sb hollow sphere	galvanic replacement	1600	435.6	/	[34]	2014
Sb_2S_3/Sb	solvothermal method	1000	387	200	[35]	2016
bundle-like Sb_2S_3 micro-structure	oxidation–sulfuration route	1000	300.5	/	[9]	2016
Sb_2S_3/lotus-pollen composites	hydrothermal method	1000 2000	436 365	/ /	[7]	2017
Sb_2S_3 nanorods wrapped in graphene sheets	hydrothermal strategy	200	610	50	[36]	2018
Sb_2S_3@C nanospheres	hydrothermal method	100	745.3	160	[37]	2018
Sb_2S_3/MMCN@ppy composite	solvothermal, sulfidation and polymerization	2000	526	/	[38]	2019
Sb_2S_3/CNT composite	ethylene glycol-mediated solvothermal process	200	443	100	[39]	2019
octahedral Sb_2O_3	method of precipitation	200	640.8	50	[40]	2019
CPC/ Sb_2S_3 composite	hydrothermal method	6000	369	/	[41]	2019
MoS_2-Sb@Sb_2S_3@C nano-tubular	in-situ thermal carbonization	10000	302.2	/	[5]	2019
S-rGO/Sb_2S_3 composite	solvothermal treatment	5000 1000	249 443	/ /	[42]	2020

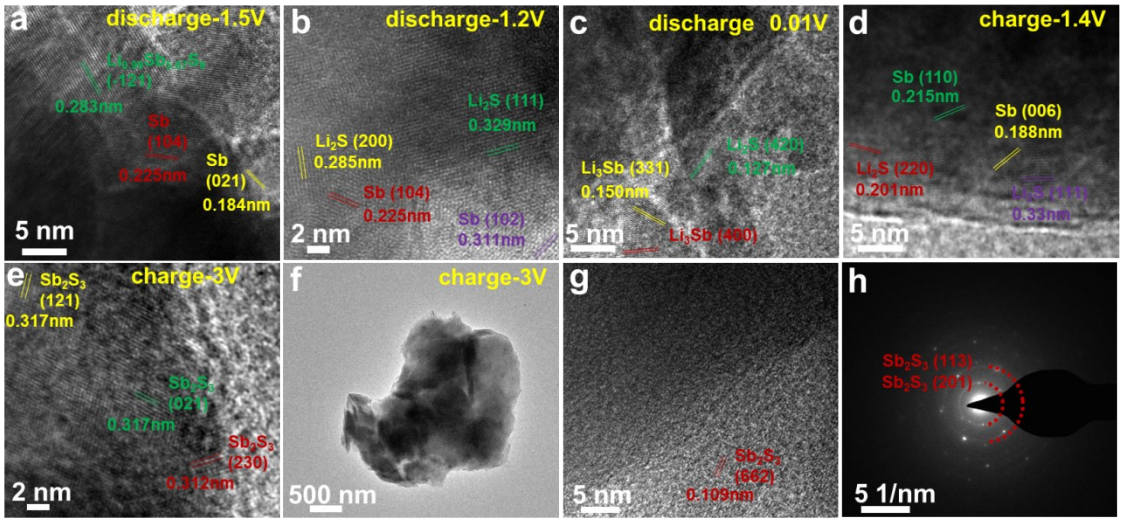

Figure S8. (a-e) HRTEM of Sb_2S_3@EG'-S at different voltage. (f) TEM, (g) HRTEM, (h) SAED of Sb_2S_3/EG-S at 3V for the first cycle.

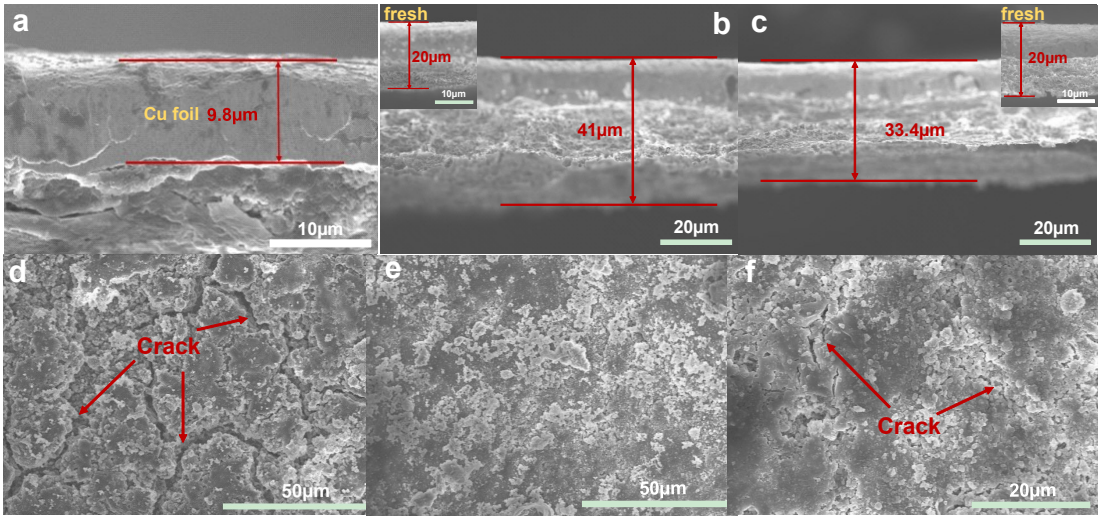

Figure S9. SEM images of two anodes. (a) copper foil, (b) Sb_2S_3/EG-S anode after 200 cycles and (C) Sb_2S_3@EG'-S after 200 cycles. Insert graphics in (b) and (c) are fresh electrodes. SEM of (d) Sb_2S_3/EG-S anode and (e) Sb_2S_3@EG'-S anode after 200 cycles. (f) Partially enlarged of (e).

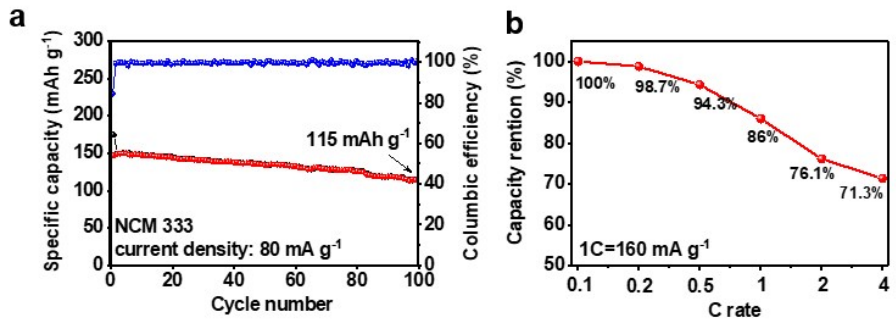

Figure S10. (a) Cycle performance of NCM333 at the current density of 80 mA g^{-1}. (b) Capacity retention of full battery at different rates.